TU Delft

Delft University of Technology

Tie-simplex parametrization for operator-based linearization for non-isothermal multiphase compositional flow in porous

Khait, M.; Voskov, D.; Konidala, G.

DOI
10.3997/2214-4609.201802183

Publication date
2018

Document Version
Final published version

Published in
16th European Conference on the Mathematics of Oil Recovery, ECMOR 2018

Citation (APA)
Khait, M., Voskov, D., & Konidala, G. (2018). Tie-simplex parametrization for operator-based linearization for non-isothermal multiphase compositional flow in porous. In D. Gunasekera (Ed.), *16th European Conference on the Mathematics of Oil Recovery, ECMOR 2018* EAGE. https://doi.org/10.3997/2214-4609.201802183

Important note
To cite this publication, please use the final published version (if applicable).
Please check the document version above.

Copyright
Other than for strictly personal use, it is not permitted to download, forward or distribute the text or part of it, without the consent of the author(s) and/or copyright holder(s), unless the work is under an open content license such as Creative Commons.

Takedown policy
Please contact us and provide details if you believe this document breaches copyrights.
We will remove access to the work immediately and investigate your claim.

This work is downloaded from Delft University of Technology.
For technical reasons the number of authors shown on this cover page is limited to a maximum of 10.

Green Open Access added to TU Delft Institutional Repository

'You share, we take care!' - Taverne project

https://www.openaccess.nl/en/you-share-we-take-care

Otherwise as indicated in the copyright section: the publisher is the copyright holder of this work and the author uses the Dutch legislation to make this work public.

ECMOR XVI
16TH EUROPEAN CONFERENCE ON THE MATHEMATICS OF OIL RECOVERY

EAGE

P053

Tie-Simplex Parametrization For Operator-Based Linearization For Non-Isothermal Multiphase Compositional Flow In Porous

M. Khait* (TU Delft), D. Voskov (TU Delft; Stanford University), G. Konidala (TU Delft)

Summary

As oil production continues worldwide, more oil fields require complex EOR methods to achieve outlined recovery factors. Reservoir engineers are dealing more often with problems involving thermal multiphase multi-component flow models tightly coupled with complex phase behavior. Such modeling implies the solution of governing laws describing mass and energy transfer in the subsurface, which in turn requires the linearization of strongly nonlinear systems of equations. The recently proposed Operator-Based Linearization (OBL) framework suggests an unconventional strategy using the discrete representation of physics. The terms of governing PDEs, discretized in time and space, which depend only on state variables, are approximated by piece-wise multilinear operators. Since the current physical state fully defines operators for a given problem, each operator can be parametrized over the multidimensional space of nonlinear unknowns for a given distribution of supporting points. Onwards, the values of operators, along with their derivatives with respect to nonlinear unknowns, are obtained from the parametrization using multilinear interpolation and are used for Jacobian assembly in the course of a simulation. Previously, the distribution of supporting points was always uniform, requiring higher parametrization resolution to provide accurate and consistent interpolation of an operator around its most non-linear regions in parameter space. In addition, when the resolution is low, the system can lose hyperbolicity causing convergence issues. In this work, we apply the prior knowledge of underlying physics to distribute the supporting points according to the tie-simplex behavior of the multiphase mixture in parameter space. The approach allows to decrease the parametrization resolution keeping the same accuracy. In addition, the OBL framework is extended to describe multisegment wells working under different controls. We test the accuracy of the developed framework for truly multi-component systems of practical interest.

Introduction

The importance of numerical modeling for subsurface-related applications can hardly be overestimated. Oil exploration and production, geothermal energy recovery, carbon dioxide sequestration have to deal with a great level of uncertainty in geological description coupled with expensive capital investment costs and high risks. Prior knowledge obtained from already developed reservoirs can't be directly applied to others. Computer modeling is an ultimate solution used to reduce the risks and improve the productivity of underground reservoirs (Aziz and Settari, 1979).

There has always been the balance between accuracy and performance for computer simulation. Over-simplified models can run in milliseconds but often divert with reality and produce meaningless results. Equally useless are super-accurate models taking too long to generate results. There should be a balance between the complexity of the model and the capability to produce the simulation results in reasonable time especially when forward simulation results are used in the inverse modeling process.

For decades, the complexity of computational devices available on the market has been increasing exponentially (Schaller, 1997). Accordingly, the complexity of reservoir simulation models has also tremendously increased. They may now require the coupled solution of equations describing different physical and chemical phenomena, leading to highly-nonlinear systems with millions of variables solved numerically (Garipov et al., 2016, 2018). The utilization of automatic differentiation is strongly suggested for this simulation frameworks to be flexible and efficient Younis (2011). However, the automatic differentiation always introduces an additional computational overhead which limits its application in inverse modeling and requires additional effort to speed it up (Moraes et al., 2017).

On the other hand, parametrization is widely used to describe the dependencies of individual model parameters on key variables. For example, multiphase fluid flow in porous media is often described through phase relative permeabilities, compressibilities, and viscosities, which are parametrized as pressure and/or saturation tables and serve as model inputs. Depending on nonlinear formulation, these parameters are evaluated as direct functions of nonlinear variables (e.g. natural formulation of Coats, 1980) or using the inversion (e.g. molar formulation of Collins et al., 1992).

In addition, parametrization can be used to improve the performance of reservoir simulation. For example, Voskov and Tchelepi (2009) proposed to describe complex multicomponent thermodynamic phase behavior with an adaptive parametrization of tie-simplexes related to thermodynamic equilibrium assumptions. Later, this idea was fully developed for compositional simulation in a parameterized tie-line space (Zaydullin et al., 2013). In this approach, the correspondent properties are evaluated in the parameter space, forming a discrete representation of complex physical relations. In the course of a simulation, the reference points from this representation are used to predict both values of properties and their derivatives by multilinear interpolation reducing expensive phase behavior computations.

Further development of the parametrization technique was proposed in Voskov (2017). The Operator Based Linearization (OBL) approach suggests parametrization of the combined operators in governing equations based on primary nonlinear unknowns - state variables. This approach was successfully applied to general purpose petroleum problems (Khait and Voskov, 2017) and geothermal problems (Khait and Voskov, 2018). In addition, it was extended for taking into account the buoyancy forces and for performing parametrization in adaptive manner (Khait et al., 2018). The method benefits not only from the increased computational performance but also due to the modular implementation of the simulation code. The latter allows to develop the multi-scale compositional transport reconstruction in Ganapathy et al. (2018) or implement an element-based formulation for reactive flow and transport in Kala and Voskov (2018) without modification of the main computational engine.

In this work, we continue to extend the capabilities of OBL approach. We describe the benefits of a tie-line-based parametrization against a uniform parametrization. Also, we implemented and tested a multi-segment well model with various well controls in the OBL-based simulation framework.

Modeling approach

In this section, we describe the governing equations and nonlinear formulations for a general compositional reservoir simulation problem.

Conservation equations

The transport equations for an isothermal system containing n_c components and n_p phases can be written as:

$$\frac{\partial}{\partial t}\left(\phi \sum_{j=1}^{n_p} x_{cj}\rho_j s_j\right) + \operatorname{div} \sum_{j=1}^{n_p} x_{cj}\rho_j \mathbf{v}_j + \sum_{j=1}^{n_p} x_{cj}\rho_j \tilde{q}_j = 0,\ c = 1,\ldots,n_c. \tag{1}$$

According to Voskov (2017), all terms of the equations can be represented as functions of coordinates in conventional three-dimensional space $\boldsymbol{\xi}$ and in parameter space $\boldsymbol{\omega}$. The former defines spatial location, whilst the latter defines physical state and, in fact, matches the set of primary nonlinear unknowns.

To describe the flow of each phase, we use Darcy's law:

$$\mathbf{v}_j = -\left(\mathbf{K}\frac{k_{rj}}{\mu_j}(\nabla \boldsymbol{p}_j - \gamma_j \nabla \boldsymbol{d})\right),\ j = 1,\ldots,n_p, \tag{2}$$

By applying a finite-volume discretization on a general unstructured mesh and backward Euler approximation in time, we can transform the conservation equations into

$$V\left((\phi\sum_j x_{cj}\rho_j s_j)^{n+1} - (\phi\sum_j x_{cj}\rho_j s_j)^{n}\right) - \Delta t \sum_{l\in \boldsymbol{L}}\left(\sum_j x_{cj}^l \rho_j^l T_j^l \Delta\psi^l\right) + \Delta t \sum_j \rho_p x_{cj} q_j = 0. \tag{3}$$

Here we neglected capillarity, gravity and used a Two-Point Flux Approximation (TPFA) with upstream weighting introducing the summation over all interfaces $\boldsymbol{L}$ connecting the control volume with its neighbors. These assumptions are not required by the method, but help to simplify the further description. Flux fluid properties $x_{cj}^l, \rho_j^l, T_j^l$ are dictated by the sign of $\Delta\psi^l$, which is equal to the difference in pressures between two control volumes sharing interface l.

Operator form of governing equations

We can re-write Eq. 3 as the component of a residual vector in an algebraic operator form

$$r_c(\boldsymbol{\xi},\boldsymbol{\omega},\mathbf{u}) = a(\boldsymbol{\xi})\left(\alpha_c(\boldsymbol{\omega}) - \alpha_c(\boldsymbol{\omega}_n)\right) - \sum_l \beta_c^l(\boldsymbol{\omega}) b^l(\boldsymbol{\xi},\boldsymbol{\omega}) + \theta_c(\boldsymbol{\xi},\boldsymbol{\omega},\mathbf{u}) = 0. \tag{4}$$

Here, we defined

$$\alpha_c(\boldsymbol{\omega}) = (1 + c_r(p - p_{ref}))\sum_j x_{cj}\rho_j s_j, \tag{5}$$

$$a(\boldsymbol{\xi}) = V(\boldsymbol{\xi})\phi_0(\boldsymbol{\xi}), \tag{6}$$

$$\beta_c(\boldsymbol{\omega}) = \sum_j x_{cj}\frac{k_{rj}}{\mu_j}\rho_j, \quad \beta_c^l(\boldsymbol{\omega}) = \begin{cases}\beta_c(\boldsymbol{\omega}) & \text{if } \Delta\psi^l > 0\\ \beta_c(\boldsymbol{\omega}^l) & \text{otherwise.}\end{cases} \tag{7}$$

$$b^l(\boldsymbol{\xi},\boldsymbol{\omega}) = \Delta t T^l(\boldsymbol{\xi})\Delta\psi^l, \tag{8}$$

$$\theta_c(\boldsymbol{\xi},\boldsymbol{\omega},\mathbf{u}) = \Delta t \sum_j \rho_j x_{cj} q_j(\boldsymbol{\xi},\boldsymbol{\omega},\mathbf{u}). \tag{9}$$

The operator α_c depends on the properties of rock and fluid, and independent of spatially distributed properties (initial porosity) as in the case of the operator a. Similarly, the divergence operator is present as a fluid-related operator β_c independent of spatially distributed properties (permeability) and the discretization-related operator b. The same approach can be applied for the well source/sink operator θ_c.

Total velocity formulation

The total velocity formulation allows analyzing of the incompressible system by segregation of elliptic and hyperbolic terms of mass conservation equation. The operator form of total velocity formulation stays equal to Eq. 4, while only convection operators require modifications:

$$\beta_c(\boldsymbol{\omega}) = \frac{\sum_j x_{cj}\frac{k_{rj}}{\mu_j}\rho_j}{\Lambda(\boldsymbol{\omega})}, \tag{10}$$

$$\Lambda(\boldsymbol{\omega}) = \sum_j \frac{k_{rj}}{\mu_j}, \quad \Lambda^l(\boldsymbol{\omega}) = \begin{cases} \Lambda(\boldsymbol{\omega}) & \text{if } \Delta\psi^l > 0 \\ \Lambda(\boldsymbol{\omega}^l) & \text{otherwise.} \end{cases} \tag{11}$$

$$b^l(\boldsymbol{\xi},\boldsymbol{\omega}) = \Delta t T^l(\boldsymbol{\xi})\Lambda^l(\boldsymbol{\omega})\Delta\psi^l \tag{12}$$

Nonlinear unknowns

The nonlinear solution of the equations 3 can be performed using different strategies (Voskov and Tchelepi, 2012). In the overall molar formulation, suggested by Collins et al. (1992), the physical state of a mixture with n_p phases and n_c components is defined by nonlinear unknowns $\boldsymbol{\omega} = [p, z_1, \ldots, z_{n_c-1}]$. The following system of equations needs to be solved at every nonlinear iteration to satisfy thermodynamic equilibrium:

$$z_c - \sum_{j=1}^{n_p} \nu_j x_{cj} = 0, \quad c = 1,\ldots,n_c, \tag{13}$$

$$f_{c1}(p,T,\boldsymbol{x}_1) - f_{cj}(p,T,\boldsymbol{x}_j) = 0, \quad j = 2,\ldots,n_p,\ c = 1,\ldots,n_c, \tag{14}$$

$$\sum_{c=1}^{n_c}(x_{c1} - x_{cj}) = 0, \quad j = 2,\ldots,n_p, \tag{15}$$

$$\sum_{j=1}^{n_p} \nu_j - 1 = 0. \tag{16}$$

This procedure is called the multiphase flash (Michelsen, 1982). For a given overall composition z_c, the solution of (13)-(16) provides molar fractions for each component x_{cj} and phase fractions ν_j. Once the multiphase flash is solved, it can provide derivatives of all properties in (3) with respect to nonlinear unknowns using the inverse theorem, see Voskov and Tchelepi (2012) for details.

Tie-line based parametrization for operator-based linearization

The OBL approach simplifies the description of fluid and rock properties by building approximation interpolants for the operators α_c, β_c and θ_c within the parameter space of a simulation problem (see Khait et al., 2018, for details). Those interpolants are then used in the course of simulation to obtain the values and partial derivatives of the operators with respect to nonlinear unknowns for Jacobian assembly. Uniform discretization of parameter space, which was used previously, proved to be a simple, efficient, and robust approach. However in this approach, approximation quality and consequently the accuracy of a simulation depend only on the number of supporting points, while their locations are prescribed blindly.

In this section, we describe tie-line-based non-uniform parametrization approach. The key idea is to use the knowledge of the thermodynamic behavior of a system to discretize the parameter space more efficiently. Using this parametrization, we can reduce interpolation error with the same parametrization accuracy (number of supporting points).

Phase behavior representation in compositional space

We show the application of tie-line parametrization for a three-component isothermal system with two hydrocarbon phases for the sake of simplicity. However, similar parametrization techniques can be extended for multi-dimensional parameter space with multiple phases (Zaydullin et al., 2013; Iranshahr et al., 2013). For each pressure within the interval of interest, we construct a ternary diagram for phase behavior representation in compositional space.

An example of such representation is shown in Fig. 1. Here, the one-phase region is shown in green and the two-phase region - in red. A tie-line is a key concept in the thermodynamical description of a multiphase multicomponent mixture at equilibrium assumptions. It is a line within the two-phase region between a bubble point B_i and a dew point D_i with equal compositions of liquid and vapor phases. Along with this line, overall compositions $\mathbf{z}$ and phase saturations $\mathbf{S}$ keep changing, but molar fractions of components within phases $\mathbf{x}$ remain constant.

All tie-lines can be extended through one-phase region to the sides of the diagram covering the sub-critical region $C_1 L_{cr} R_{cr} C_2$ (see Fig. 1). If a critical point z_{cr} exists for the system under given p, T, then the tie-line which passes through that point has zero length and is called a critical tie-line. The part of the one-phase region which is above the extended critical tie-line $L_{cr}R_{cr}$ is called super-critical region. The approach provides separate parametrization treatment for these regions. If the critical point doesn't exist for given p, T then we assume that the sub-critical region covers the entire compositional space $[C_1, C_2, C_3]$.

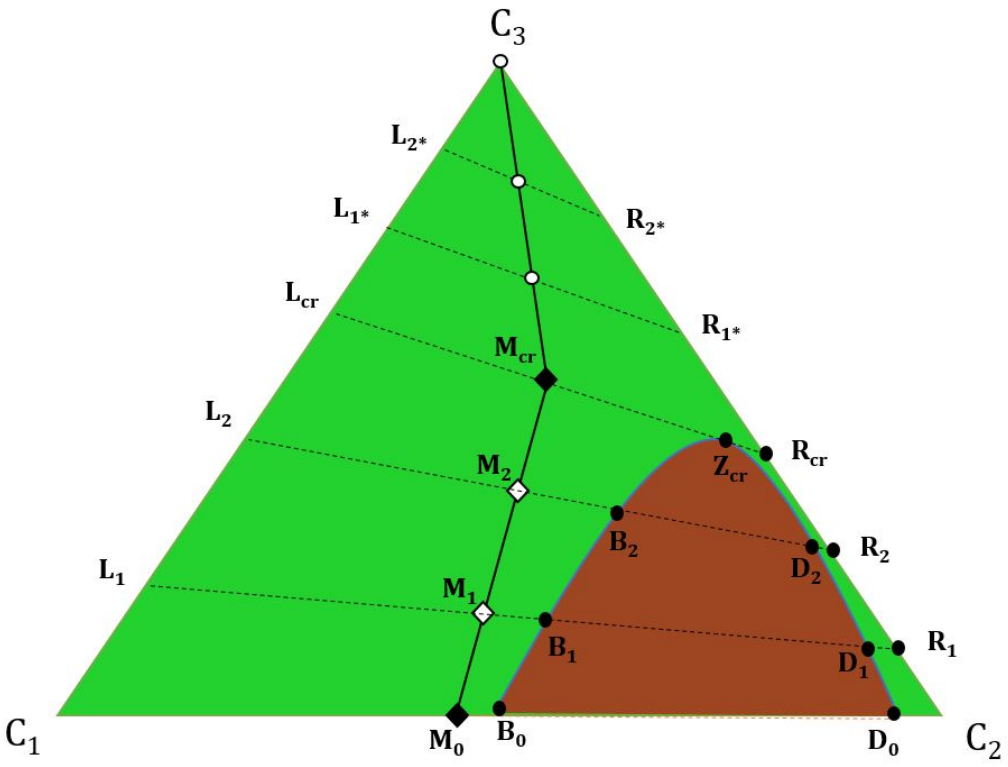

Figure 1 *Tie-line based compositional space parametrization.*

Sub-critical region parametrization

We use an extension of tie-lines to parametrize the entire sub-critical region. First, we obtain the number of intermediate tie-lines between the critical $L_{cr}R_{cr}$ and the base (longest) C_1C_2 tie-lines based on the distance between their midpoints M_{cr}, M_0 and discretization parameter Δx:

$$n_{it} = \left\lceil \frac{|M_0 M_{cr}|}{\Delta x} \right\rceil . \tag{17}$$

Next, we split M_0M_{cr} into $n_{it}+1$ equal segments and get the midpoints M_i of intermediate extended tie-lines L_iR_i, where $i = 1 \dots n_{it}$. Now, for every intermediate tie-line, we place supporting points at L_i, B_i, D_i, and R_i. Naturally, we also place them at $C_1, B_0, D_0, C2, L_{cr}, Z_{cr}$, and R_{cr}. The segments L_iB_i, B_iD_i, and D_iR_i are evenly divided by the fixed number of supporting points into subsegments, similarly to M_0M_{cr}. As the result, each subsegment becomes shorter than Δx. Segments $C_1B_0, B_0D_0, D_0C_2, L_{cr}Z_{cr}$, and $Z_{cr}R_{cr}$ are treated in the same way.

Super-critical region parametrization

The super-critical region can't be parameterized using tie-lines, because they neither exist nor extend there. Instead, we apply a uniform parametrization with grid-lines parallel to the critical tie-line. First, we determine the number of such lines:

$$n_{il} = \left\lceil \frac{|M_{cr}C_3|}{\Delta x} \right\rceil . \tag{18}$$

Then, we split each of the segments $L_{cr}C_3, R_{cr}C3$ into $n_{il}+1$ equal subsegments. Finally, we place supporting points at C_3, L_i^*, R_i^* and along segments $L_i^*R_i^*$, so that the segments become sliced into the equal subsegments shorter than Δx. Later, we test tie-line-based parametrization against a uniform parametrization proposed in Voskov (2017); Khait and Voskov (2017).

Multi-segment wells

In this section, we briefly describe the concept of multi-segment well and introduce additional OBL operators to cover the two sets of well controls used in practice.

Space discretization

Following the general unstructured grid framework, a well is discretized by a set of well segment control volumes, chained together by connections with high transmissibility. Any well segment can also be connected with an arbitrary number of reservoir control volumes, representing well perforation. For well discretization, we use connection-based approach, suggested by Lim et al. (1995). Each perforation is characterized by geometrical transmissibility representing the connectivity of corresponding well segments to the reservoir, also referred to as well index. In addition, the top well segment is also connected to a ghost control volume, which has exactly one connection and is used as a placeholder for well control equations, see details in Jiang (2007).

A simple example is shown in Fig. 2. Reservoir control volumes are shown in gray; well control volumes including the top segment w_1 - in blue; well ghost control volume w_0 - in red. The interface between w_0 and w_1 is denoted as w. Black arrows represent connections between reservoir control volumes; blue arrows - perforation connections; red arrows - intra-well connections. All well control volumes are considered as the extensions of a reservoir and treated exactly the same way during Jacobian assembly, except for w_0. Each well segment is defined by a volume dependent on a wellbore diameter and a segment length, while porosity of the control volume is set to 1. The flow in the multi-segment well is following the homogeneous flow in an idealized tube without roughness and slip (Jiang, 2007).

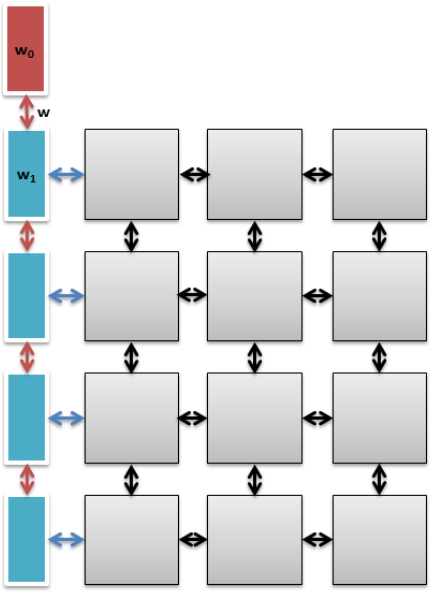

Figure 2 *Example of multi-segment well discretization for structured reservoir.*

BHP well control

One of the two most common controls for wells in reservoir simulation is fixed bottom hole pressure. The following system of equations is applied to w_0 control volume instead of Eq. 4 in order to maintain target pressure p^{target}:

$$p - p^{target} = 0, \tag{19}$$

$$z_c - z_c^{up} = 0, \quad c = 1,\ldots,n_c-1, \quad z_c^{up} = \begin{cases} z_c^{inj} & \text{for injector} \\ z_c^{w_1} & \text{for producer} \end{cases} \tag{20}$$

Rate well control

Another common way to define well regime is to specify volumetric phase rate at surface conditions. In order to parametrize this rate, we first define the state at separator (or surface) conditions using the overall composition of the flux β_c^w over interface w, which is evaluated according to 7:

$$\boldsymbol{\omega}^{SC} = [p^{SC}, T^{SC}, \frac{\beta_1^w}{\sum_c \beta_c^w}, \ldots, \frac{\beta_{n_c-1}^w}{\sum_c \beta_c^w}] \tag{21}$$

Now, we can obtain target rate introducing rate operator $\zeta_j(\boldsymbol{\omega})$:

$$Q_j = \frac{b^w \sum_c \beta_c^w}{dt} \frac{S_j(\boldsymbol{\omega}^{SC})}{\rho_t(\boldsymbol{\omega}^{SC})} = \frac{b^w}{dt}\zeta^w(\boldsymbol{\omega}), \quad \zeta_j^w(\boldsymbol{\omega}) = \begin{cases} \zeta_j(\boldsymbol{\omega}) & \text{for injector} \\ \zeta_j(\boldsymbol{\omega}^w) & \text{for producer} \end{cases} \tag{22}$$

Next, we write down equations for control volume w_0 to maintain target rate Q_j^{target}:

$$\frac{b^w}{dt}\zeta_j^w(\boldsymbol{\omega}) - Q_j = 0, \tag{23}$$

$$z_c - z_c^{up} = 0, \quad c = 1,\ldots,n_c-1, \quad z_c^{up} = \begin{cases} z_c^{inj} & \text{for injector} \\ z_c^{w_1} & \text{for producer} \end{cases} \tag{24}$$

Numerical results

Here we present the numerical experiments using the simulation framework based on OBL.

Tie-line based parametrization

The quality of a parametrization approach can be assessed using the accuracy of the interpolator built on that parametrization. Previously, the piecewise multilinear interpolation was used, since supporting points were distributed over parameter space in a uniform manner. This condition is no longer valid with the tie-line-based parametrization approach. Therefore, in order to compare the tie-line-based parametrization and uniform parametrization, we apply the Delaney triangulation to the set of supporting points and then use a barycentric interpolation based on triangular simplices in both cases (Weiser and Zarantonello, 1988; Zaydullin et al., 2013). The accuracy of an interpolator I can be checked directly at any point of parameter space by absolute difference between interpolated value and true value. A generalized error can be obtained by multiple application of this procedure at every point in set $\boldsymbol{\Omega}$, covering densely the entire parameter space: The error is computed in every point of compositional space as L_2 norm of operator for components:

$$||E_\alpha||_i = \frac{\sqrt{\sum_{c=1}^{n_c}(I_{\alpha_c^D}(\boldsymbol{\omega}_i) - \alpha_c(\boldsymbol{\omega}_i))^2}}{\max_{j,c}|\alpha_c(\boldsymbol{\omega}_j)|}. \tag{25}$$

Here, $I_{\alpha_c^D}$ is the interpolant of operator α_c in discrete parameter-space $\boldsymbol{\Omega}^D$, c corresponds to the component and $\boldsymbol{\omega}_i$ corresponds to the distributed points in the compositional space.

We demonstrate the results of the approach modeling fluid mixture of CO_2, NC_4, and C_{10} at three particular pressures of 20, 60, and 100 bars, while the temperature is fixed at 345°K.

Phase diagrams for the mixtures at all 3 pressures are shown in Fig. 3. In Fig. 3,a, the two-phase region occupies almost the entire parameter space. The Fig. 3,b shows the phase behavior at $p = 60$ bars. Here, two-phase region has reduced, but the extension of two-phase still parameterize the entire compositional space. Similar diagram was generated for $p = 100$ bars in Fig. 3,c. Here, the two-phase and entire sub-critical regions occupy a smaller portion of the compositional space and the large portion of space is present in critical region.

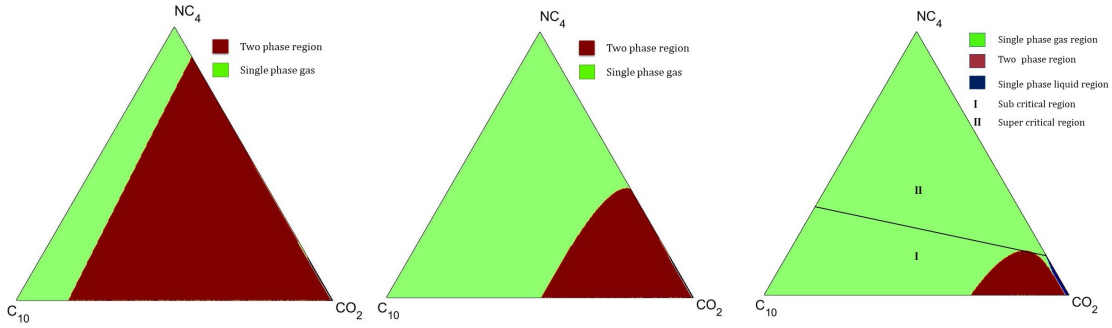

Figure 3 *Ternary diagram for the system CO_2,NC_4,C_{10} at p = 20, 60 and 100 bars, $T = 345°K$.*

Fig. 4 and Fig. 5 show the norm of combined operators α and β at different pressures respectively. These figures confirm that the thermodynamic properties of the system dictate the behavior of accumulative and flux operators. The border between one-phase and two-phase regions accounts for the most abrupt changes in operators values. With growing pressure, the two-phase region shrinks and the nonlinearity increases, especially for the convection operator β.

In Fig. 6 and 7, we demonstrate the normalized interpolation errors for α operator $E_\alpha(\boldsymbol{\omega})$ in case of adaptive and uniform parametrization respectively. The correspondent mesh is also shown for both

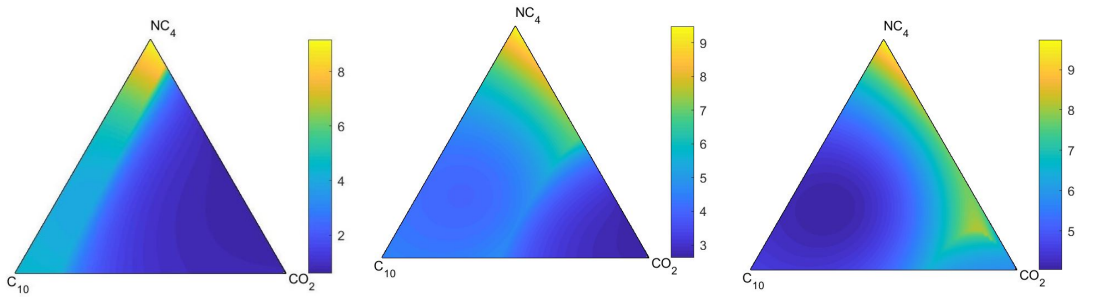

Figure 4 *Euclidian norms of accumulation operator α at $p = 20$, 60 and 100 bars.*

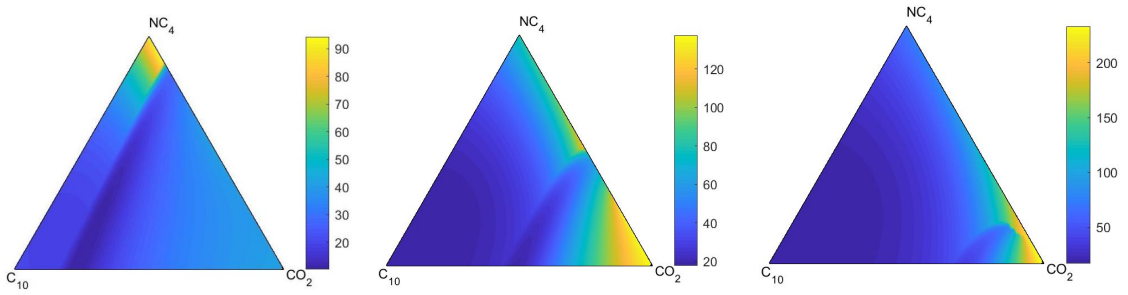

Figure 5 *Euclidian norms of convection operator β at $p = 20$, 60 and 100 bars.*

types of parametrization. It can be clearly seen how the tie-line-based mesh adapts to the shape of the two-phase region.

For the meaningful comparison of errors, the number of supporting points in uniform and adaptive parametrizations should be equivalent. This is easy to control in uniform parametrization but more difficult in adaptive, since the number and density of supporting points depend on the form of the two-phase region. In the following comparison, we generate adaptive parametrization first with fixed parameters. Next, we select the resolution of uniform parametrization to match the number of points in adaptive parametrization as close as possible. This approach lets us compare the errors consistently.

The number of points for adaptive parametrization at pressures $p = 20$, 60 and 100 bars is 46, 36 and 51 points respectively. To compare the errors, the resolution of uniform parametrization was tuned to generate 45, 36 and 55 points for these pressures respectively. Based on analysis of the error map, the main error is concentrated at the boundary of the two-phase region and more pronounced for the uniform parametrization. In case of convection operator β, the error in adaptive parametrization is closer to the errors in uniform parametrization, see Fig. 8 and Fig. 9 for adaptive and uniform parametrization respectively.

The maximum errors of a combined operator are considered for sensitivity analysis as

$$\|E_\alpha\| = \max_i \|E_\alpha\|_i. \tag{26}$$

The variation of error with the increase in the number of supporting points is shown on semi-log plot on the x-axis. Five intervals are chosen between parameterizing distance $\Delta x = 0.1$ and $\Delta x = 0.01$. Since the nonlinearity is strongly correlated with the two-phase shape, the error behaves non-monotonically at higher pressure for both parametrizations. However, in the most cases, the error at lower resolutions for the adaptive mesh is smaller than the error for the uniform mesh. At lower Δx, the difference in errors between uniform and adaptive mesh reduces since the proximity between supporting points increases.

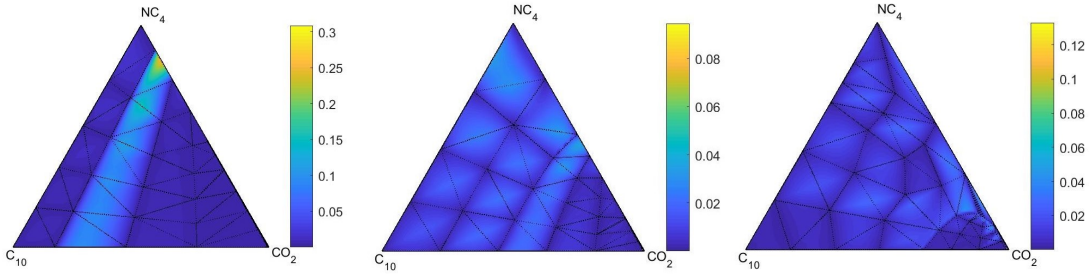

Figure 6 *Errors for adaptive parametrization of accumulation operator α at $p = 20$, 60 and 100 bars.*

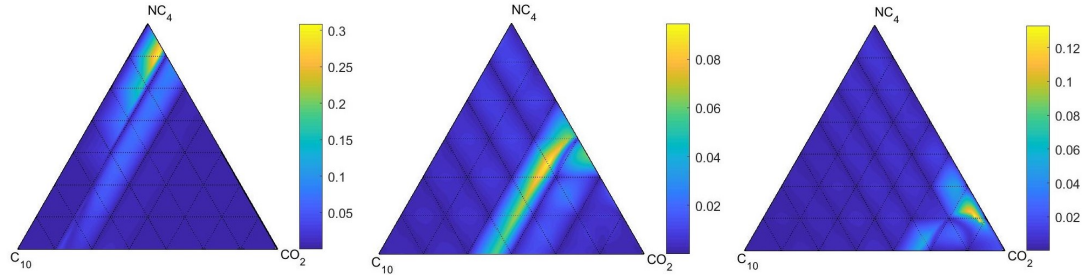

Figure 7 *Errors for uniform parametrization of accumulation operator α at $p = 20$, 60 and 100 bars.*

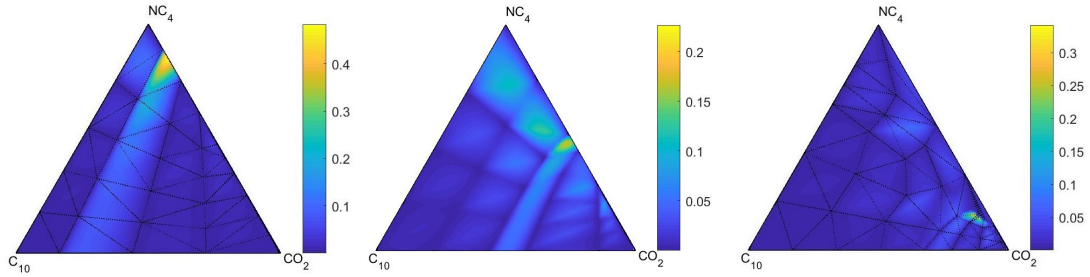

Figure 8 *Errors for adaptive parametrization of convection operator β at $p = 20$, 60 and 100 bars.*

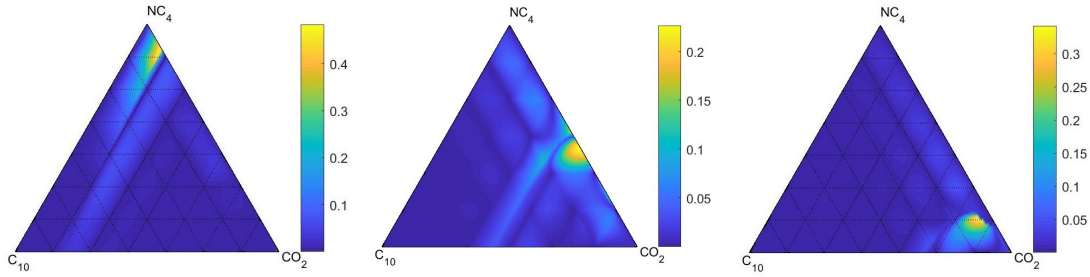

Figure 9 *Errors for uniform parametrization of convection operator β at $p = 20$, 60 and 100 bars.*

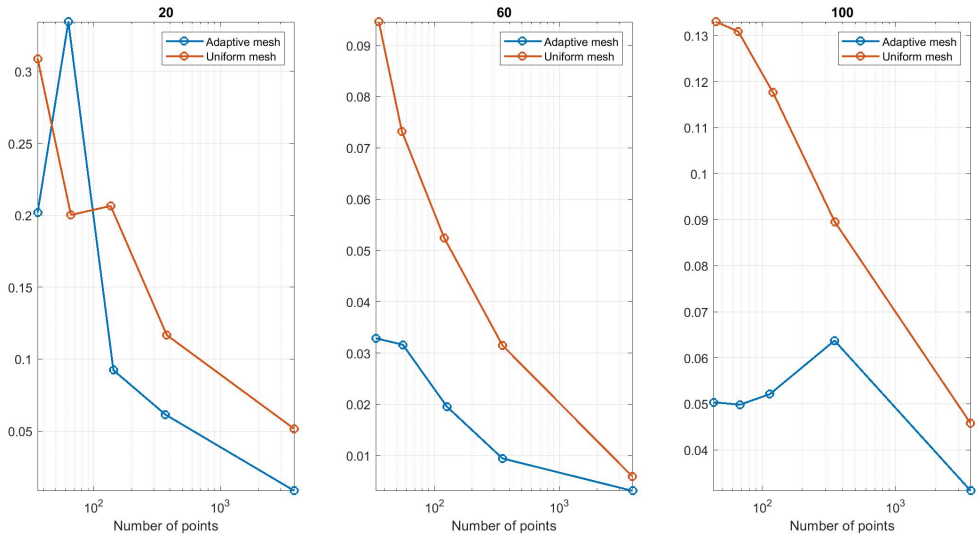

Figure 10 *Mean error comparison for accumulation operator with various parametrization resolutions at $p = 20$, 60 and 100 bars.*

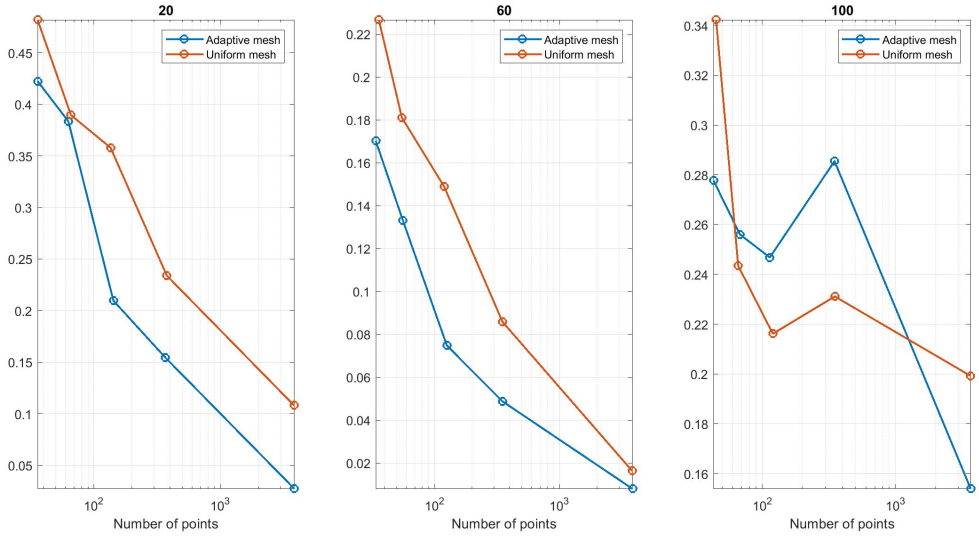

Figure 11 *Mean error comparison for flux operator with various parametrization resolutions at $p = 20$, 60 and 100 bars.*

Multi-segment wells

Another source of error comes from operators involved into the approximation of properties for well controls. Multi-segment wells provide the most accurate solution when cross-flow effects coupled with complex phase behavior occur in the reservoir model. In order to mimic these conditions, we took a synthetic model comprised of three layers with lateral permeabilities of K_{xy} =100, and 500 mD, while vertical permeability was set as $K_z = \frac{K_{xy}}{100}$. Each layer consisted of 10x10 grid blocks of 100x100x10m with the porosity of 25%. The initial oil was made of 3 components C_1, C_4, and C_{10} at corresponding compositions: 1% of methane, 35% of n-butane, and 64% of n-decane. The description of phase behavior and properties was based on Peng-Robinson Equation of State (Peng and Robinson, 1976).

Two vertical multi-segment wells with three segments each were placed at the opposite corners of the model. Each segment was connected to the correspondent layer with different well indexes of 10, 20 and 30. We injected a mixture of 99% of C_1 and 1% of C_4 at a constant gas rate $Q_g = 1.5e5\ sm^3/day$. The production well operates at a constant oil rate $Q_o = 800\ sm^3/day$ with minimum BHP constraint of 10 bar. In order to model single-phase gas injection into a single-phase liquid, we set the initial pressure was $P_0 = 60$ bars and temperature $T_0 = 77^o$ C. The simulation period was 4000 days.

The comparison between OBL simulator denoted as DARTS, and ADGPRS with multi-segment well model is shown in Fig. 12, 13. The two results match very well. Injector BHP climbs up due to gas compressibility till breakthrough happens after roughly 1600 days of simulation, as it can be seen from Fig. 12. After that injection pressure rapidly drops, while producer can't satisfy oil rate control anymore after roughly 2300 days of simulation and therefore switches to BHP constraint of 10 bar.

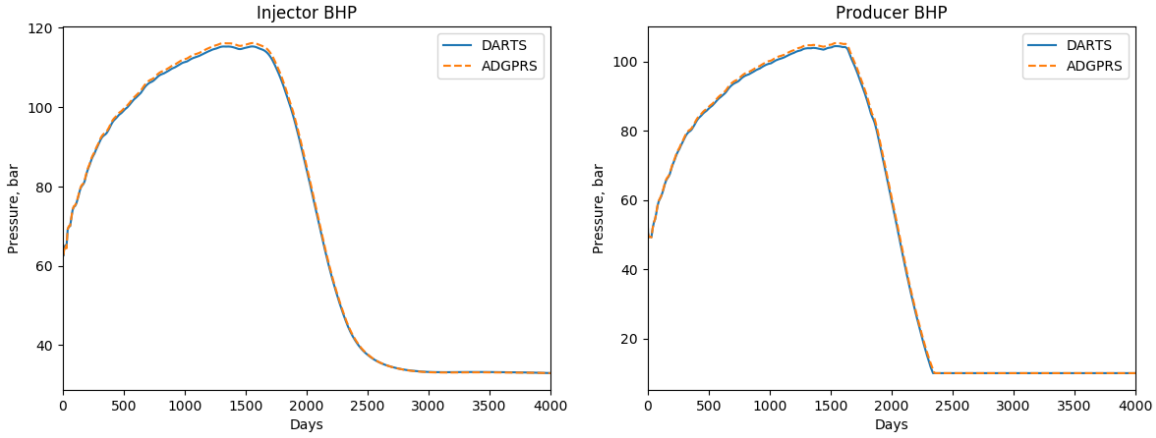

Figure 12 *BHP for injector and producer provided by DARTS and ADGPRS.*

Producer gas and oil rates comparisons are shown in Fig. 13. There is a very good match between DARTS and ADGPRS results. Producer gas rate starts at 0, then rapidly increases after the breakthrough and falls back after the producer switches to BHP control. Production oil rates provided by DARTS and ADGPRS multi-segment well model (denoted as ADGPRS_ms) match well. The results provided by ADGPRS standard well model, denoted as ADGPRS_std, underestimates oil production after the breakthrough and illustrates the substantial difference between the two well models in this case.

In order to test the same physical set up in a highly heterogeneous reservoir, we took the top layer of SPE10 test case (Christie and Blunt, 2001) and applied inverted 5 spot well pattern. The reservoir initial physical state and injection mixture were the same as in the previous case. Injection well started with BHP control at 180 bar, and after 500 days switched to gas rate control $Q_g = 2300\ sm^3/day$ with maximum BHP constraint of 199 bar. Production wells, placed at the corners, operated with gas rate control $Q_g = 200\ sm^3/day$ with minimum BHP constraint of 30 bar. The simulation period was 2500 days.

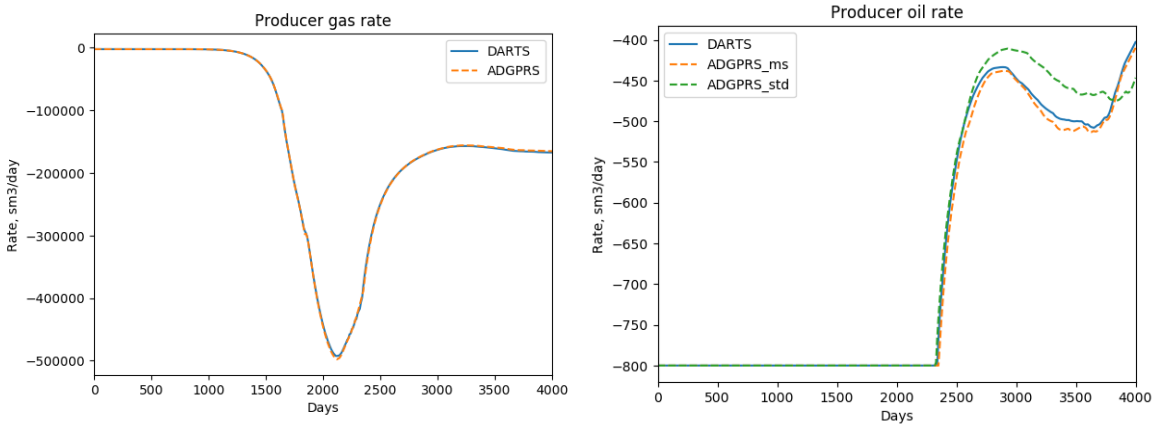

Figure 13 *Producer oil and gas rates provided by DARTS and ADGPRS.*

Figs. 14, 15, 16 , 17 demonstrate close match between DARTS and ADGPRS results. Injection well switched to gas rate control after 500 days of simulation and reached BHP limit by roughly 1900th day, as it can be seen in Fig. 14. P1 and P2 production wells happened to perforate low permeable reservoir area producing negligible amounts of fluids, so we omit their results. BHP for P3 and P4 are shown in Fig. 15. For P3 it remains constant throughout the simulation, while for P4 it starts raising after 1500 days of simulation - the well switches to gas rate constraint after the breakthrough. This is confirmed by Figs. 16 and 17. Oil production rate immediately decreases while gas production rate increases till it's limit of $Q_g = 200\ sm^3/day$ once the breakthrough is reached for P4. A small increase of gas production rate by the end of simulation indicates the breakthrough for P3 well.

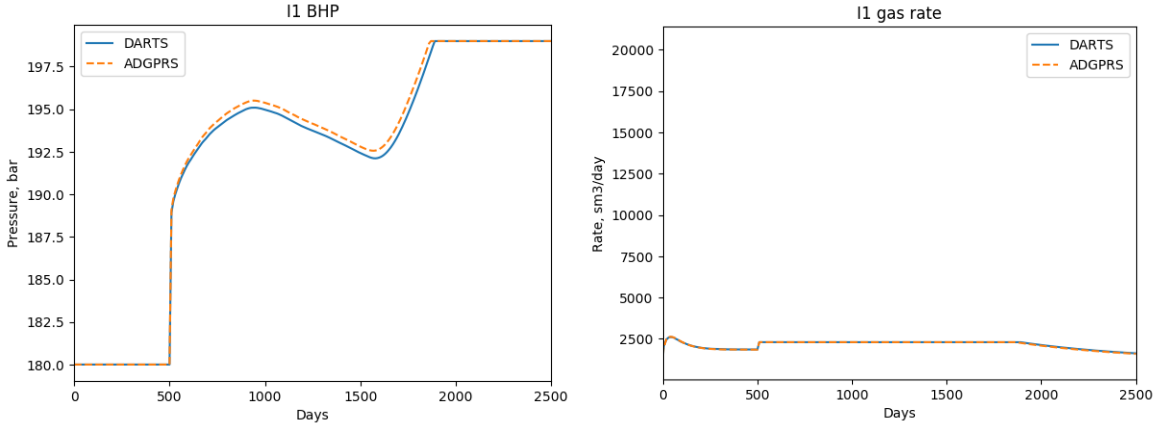

Figure 14 *Injector BHP and gas rate provided by DARTS and ADGPRS.*

Conclusions

The Operator-Based Linearization approach proves to be an effective way to deal with complex multiphase flow in porous media. In this work, we extended the OBL approach farther and improved the approximation accuracy by introducing adaptive parametrization in the physical space of a problem. In particular, for a compositional problem with three components, we have placed the supporting points along with a discrete set of tie-lines in the two-phase region. Next, we performed triangulation and applied the reconstruction of OBL operators based on barycentric interpolation. This approach was tested for the range of pressures and demonstrated a reasonable improvement comparing to the uniform parametrization and piecewise multilinear interpolation.

In addition, we extended the OBL approach and introduce a multi-segment well model. We utilized conventional accumulation and flow operators to describe the flow between segments. For rate controls,

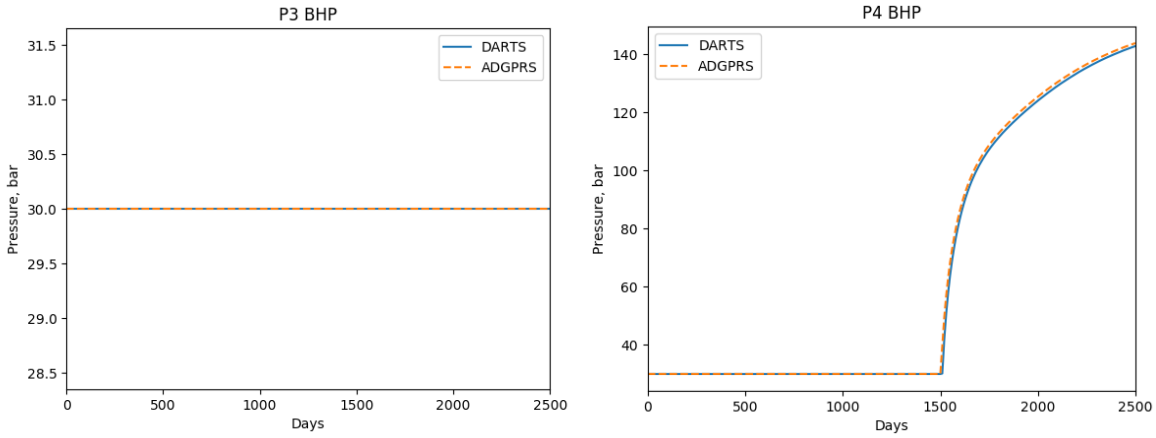

Figure 15 *P3 and P4 BHP provided by DARTS and ADGPRS.*

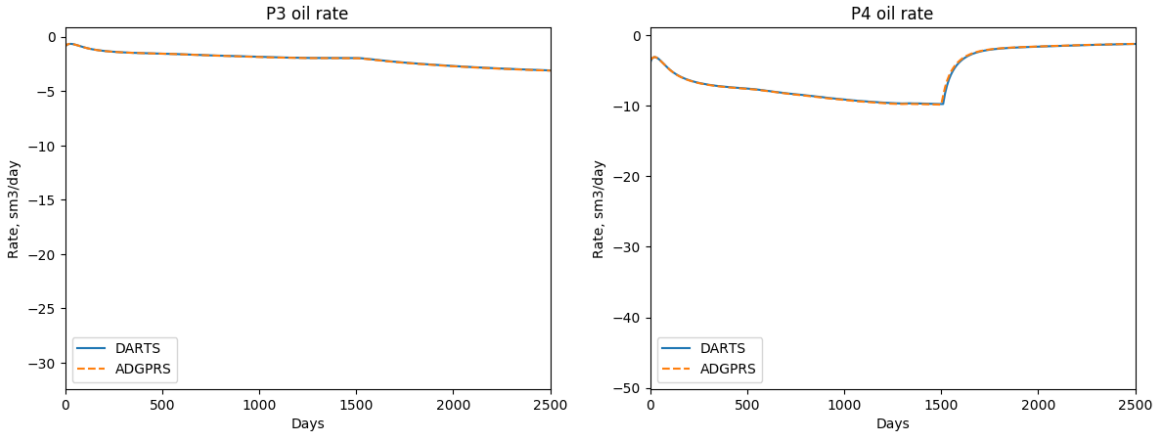

Figure 16 *P3 and P4 oil rates provided by DARTS and ADGPRS.*

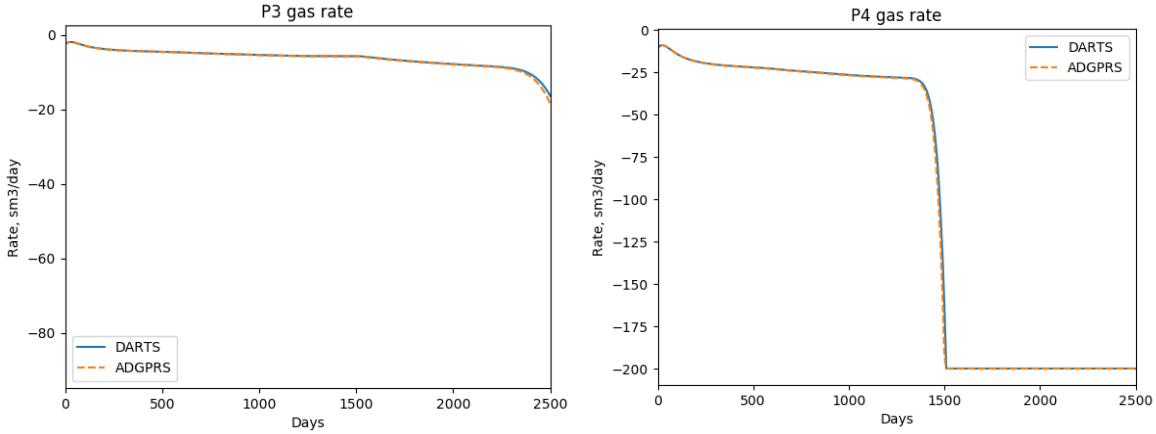

Figure 17 *P3 and P4 gas rates provided by DARTS and ADGPRS.*

we introduced additional sets of phase rate operators which depend on both reservoir and separator conditions. These operators translated the solution at the last segment into the rate control or constraint. We tested our multi-segment model for several realistic scenarios and demonstrated a good match with the reference results. The future work will include an extension of adaptive parametrization to multiple components and farther improvement of the parametrization accuracy.

Nomenclature

$\boldsymbol{d}$	depths (positive downwards)
$\boldsymbol{p}_j$	pressures of phase j
γ_j	gravity term for phase j
μ_j	viscosity of phase j
ρ_j	molar density of phase j
$\tilde{q}_j$	rate of phase j per unit volume
$\mathbf{v}_j$	velocities of phase j
k_{rj}	relative permeability of phase j
q_j	rate of phase j
s_j	saturation of phase j
x_{cj}	molar fraction of component c in phase j
$\mathbf{K}$	permeability tensor
α	accumulation operator
β	flux operator
$\boldsymbol{\xi}$	spatial coordinate
$\Delta\psi^l$	pressure difference across interface l
ν_j	overall molar fraction of phase j
$\boldsymbol{\omega}$	state coordinate (nonlinear unknowns)
$\boldsymbol{\omega}^l$	state coordinate of the adjacent across interface l control volume
$\boldsymbol{\omega}_n$	state coordinate on the previous time step
ϕ	porosity
θ	source/sink operator
$\mathbf{u}$	well control variables
$\boldsymbol{x}_j$	molar fractions of components within phase j
ζ	phase rate operator
f_{cj}	fugacity of component c within phase j
q_j	source of phase j
T^l	the geometric part of transmissibility across interface l
T_j	transmissibility of phase j
V	volume of control volume
z_c	overall molar fraction of component c

Acknowledgements

We acknowledge the Stanford University Petroleum Research Institute for Reservoir Simulation (SUPRI-B) program for the permission to use ADGPRS. We also thank Oleg Borschuk for his help with the algebraic multigrid linear solver.

References

Aziz, K. and Settari, T. [1979] *Petroleum Reservoir Simulation*. Applied Science Publishers.

Christie, M. and Blunt, M. [2001] Tenth SPE comparative solution project: A comparison of upscaling techniques. *SPE Reservoir Eval. & Eng.*, **4**(4), 308–316.

Coats, K. [1980] An Equation of State Compositional Model. *Soc. Petrol. Eng. J.*, **20**, 363–376.

Collins, D., Nghiem, L., Li, Y.K. and Grabenstetter, J. [1992] Efficient approach to adaptive-implicit compositional simulation with an equation of state. *Soc. Petrol. Eng. J.*, **7**(2), 259–264.

Ganapathy, C., Chen, Y. and Voskov, D. [2018] Multiscale Reconstruction of Compositional Transport. In: *ECMOR 2018-16th European Conference on the Mathematics of Oil Recovery*.

Garipov, T., Karimi-Fard, M. and Tchelepi, H. [2016] Discrete fracture model for coupled flow and geomechanics. *Computational Geosciences*, **20**(1), 149–160.

Garipov, T., Tomin, P., Rin, R., Voskov, D. and Tchelepi, H. [2018] Unified Thermo-Compositional-Mechanical Framework for Reservoir Simulation. *Computational Geosciences*.

Iranshahr, A., Voskov, D. and Tchelepi, H. [2013] Tie-simplex based compositional space parameterization: Continuity and generalization to multiphase systems. *AIChE J*, **59**(5), 1684–1701.

Jiang, Y. [2007] *Techniques for Modeling Complex Reservoirs and Advanced Wells*. PhD Thesis, Stanford University.

Kala, K. and Voskov, D. [2018] Parametrization of element balance formulation in reactive compositional flow and transport. In: *ECMOR XV-16th European Conference on the Mathematics of Oil Recovery*.

Khait, M. and Voskov, D. [2018] Operator-based linearization for efficient modeling of geothermal processes. *Geothermics*, **74**, 7–18.

Khait, M., Voskov, D. et al. [2018] Adaptive Parameterization for Solving of Thermal/Compositional Nonlinear Flow and Transport With Buoyancy. *SPE Journal*.

Khait, M. and Voskov, D.V. [2017] Operator-based linearization for general purpose reservoir simulation. *Journal of Petroleum Science and Engineering*, **157**, 990–998.

Lim, K.T. et al. [1995] A new approach for residual and jacobian arrays construction in reservoir simulators. *SPE Computer Applications*, **7**(04), 93–96.

Michelsen, M. [1982] The isothermal flash problem: Part II. Phase-split calculation. *Fluid Phase Equilibr.*, **9**, 21–40.

Moraes, R.J.d., Rodrigues, J.R., Hajibeygi, H. and Jansen, J.D. [2017] Multiscale gradient computation for flow in heterogeneous porous media. *Journal of Computational Physics*, **336**, 644–663.

Peng, D.Y. and Robinson, D.B. [1976] New two-constant equation of state. *Ind Eng Chem Fundam*, **15**(1), 59–64.

Schaller, R.R. [1997] Moore's law: past, present and future. *IEEE spectrum*, **34**(6), 52–59.

Voskov, D. and Tchelepi, H. [2009] Tie-simplex based mathematical framework for thermodynamical equilibrium computation of mixtures with an arbitrary number of phases. *Fluid Phase Equilibria*, **283**(1-2), 1–11.

Voskov, D.V. [2017] Operator-based linearization approach for modeling of multiphase multi-component flow in porous media. *Journal of Computational Physics*, **337**, 275–288.

Voskov, D.V. and Tchelepi, H.A. [2012] Comparison of Nonlinear Formulations for two-phase multi-component EoS based simulation. *J. Petrol. Sci. Eng.*, **82-83**, 101–111.

Weiser, A. and Zarantonello, S. [1988] A note on piecewise linear and multilinear table interpolation in many dimensions. *Math Comput*, **50**(181), 189–196.

Younis, R. [2011] *Modern Advances in Software and Solution Algorithms for Reservoir Simulation*. Ph.D. thesis, Stanford University.

Zaydullin, R., Voskov, D. and Tchelepi, H. [2013] Formulation and solution of compositional displacements in tie-simplex space. In: *SPE Reservoir Simulation Symposium 2013*, 2. 1268–1282.